Improving the Quality of 3D-QSAR by Using Flexible-Ligand Receptor Models

Jianfeng Pei,[†,‡] Hao Chen,[†,‡] Zhenming Liu,[†,‡] Xiaofeng Han,[†,‡] Qi Wang,[†,‡] Bin Shen,[§] Jiaju Zhou,[||] and Luhua Lai*[,†,‡]

State Key Laboratory for Structural Chemistry of Stable and Unstable Species, College of Chemistry and Molecular Engineering and Center for Theoretical Biology, Peking University, Beijing 100871, China, and Computer Network Information Center and Institute of Process Engineering, Chinese Academy of Sciences, Beijing 100080, China

Received May 19, 2005

To address the problems associated with molecular conformations and alignments in the 3D-QSAR studies, we have developed the Flexible Ligand − Atomic Receptor Model (FLARM) 2.0 method. The FLARM 2.0 method has three unique features as compared to other pseudoreceptor model methods: (1) the training ligands are flexibly optimized inside the receptors to achieve minimal docking energies; (2) the receptor atoms are spatially moveable in the process of genetic evolving in order to avoid improper initial receptor shapes; and (3) void receptor sites are specially favored in order to obtain open receptor models that allow large gaps. Advantages of an open model include less noise information, a smaller risk of overfitting, and ease of locating the key interaction sites. The latter two features, inherited from the previous FLARM 1.0 method, can improve the predictive ability of the 3D-QSAR models, while the first feature is newly implemented to relieve the uncertainty caused by improper conformation and alignment. Three FLARM 2.0 case studies were performed, and the results show that FLARM 2.0 models are highly predictive and robust. FLARM 2.0 pseudoreceptor models can correspond well with the pharmacophore models and/or the binding sites of the real protein receptors.

INTRODUCTION

Though a structural genomics era has begun, scientists today still find it hard and time-consuming to solve the three-dimensional (3D) structure of a certain drug target, especially when the drug target is membrane-related. However, it is often easier for medicinal chemists to synthesize a set of molecules acting upon a particular receptor protein target and measure their bioactivity date. With these molecules and their bioactivity data, ligand-based drug design methods, for example, the quantitative structure−activity relationships (QSAR) method can be used to derive QSAR models and pharmacophore models that can further guide the design and discovery of new ligands with high bioactivity.

As a type of 3D-QSAR method, the methods based on the strategy of constructing hypothetical receptor models have been successfully developed in the last couple of decades. In 1994, Jain et al. reported a pseudoreceptor model consisting of receptor shape factors and van der Waals (VDW) interactions to predict the odor of flavorants,[1] and Walters and Hinds proposed an approach (GERM) using pseudoatoms mimicking the protein atoms to construct receptor models.[2] In 1995, Hahn developed the receptor surface model by using grid points describing four types of interactions—electrostatic, hydrophobic, hydrogen bond, and VDW, in the receptor model 3D surface surrounding the set of ligands.[3,4] In the same year, Vedani and co-workers developed a method to derive pseudoreceptor models directly using the fragments from amino acids.[5] They also developed in 1998 the quasiatomistic receptor model, which is populated with atomistic properties (hydrogen bonds, salt bridges, aromatic and aliphatic regions, solvent).[6] For these receptor model methods, like other 3D-QSAR methods, a set of ligand structures together with their bioactivities were required to deduce and train the receptor models by using different algorithms such as genetic algorithms or neural network algorithms.

In 1997, Chen et al. put forward a pseudoatomic receptor model (PARM) algorithm that was based on GERM approach to predict bioactivity.[7,8] The improvement of PARM on GERM is the use of the cross-validated R^2 instead of the conventional R^2 to reduce the chance of overfitting.[7] In our earlier work, we updated PARM to a novel flexible atomic receptor model (FLARM 1.0) method.[9] Compared to the previous receptor model methods, FLARM 1.0 has two prominent improvements: (1) Flexible receptor models − FLARM introduced the concept of a flexible receptor model in order to avoid the bias of the fixed receptor shape that is sensitive to the ensemble of the training set. All the atoms in a FLARM receptor model are spatially moveable in the process of genetic evolving to construct the receptor models. (2) Open receptor models − Usually, in a receptor model generated by the conventional methods, ligands are fully closed. But in the real world, there are many cases in which ligands are only partly enwrapped in receptors. FLARM can produce open receptor models that allow large gaps and may

* Corresponding author phone: (86)-010-62757486; fax: (86)-010-62751725; e-mail: lhlai@pku.edu.cn. Corresponding author address: College of Chemistry and Molecular Engineering, Peking University, Beijing 100871, China.

† College of Chemistry and Molecular Engineering, Peking University.

‡ Center for Theoretical Biology, Peking University.

§ Computer Network Information Center, Chinese Academy of Sciences.

|| Institute of Process Engineering, Chinese Academy of Sciences.

10.1021/ci050203c CCC: $30.25
Published on Web 09/21/2005

Table 1. Receptor Atom Types and Parameters

atom type code	atom type	E_{min} (kcal/mol)	atomic radius (Å)	partial atomic charge[a]	H-bond property[b]	occurrence weight	occurrence rate in the natural binding sites (%)
1	void	0.0	0.0	0.0	N	800	
2	H (nonpolar)	0.042	1.5	0.00	N	160	40.0
3	H (polar)	0.042	1.5	0.25	D	36	9.1
4	H (charged)	0.042	1.5	0.35	D	8	1.7
5	C (aliphatic)	0.107	1.7	0.00	N	70	17.5
6	C (aromatic)	0.107	1.7	0.00	N	36	9.1
7	C (charged)	0.107	1.7	0.35	N	26	6.3
8	N (amide)	0.095	1.55	−0.40	N	24	5.7
9	N (amine)	0.095	1.55	−0.30	A	4	1.1
10	N (charged)	0.095	1.55	−0.40	N	1	0.15
1	O (carbonyl)	0.116	1.52	−0.50	A	22	5.5
12	O (hydroxyl)	0.116	1.52	−0.60	A	6	1.4
13	O (charged)	0.116	1.52	−0.65	A	8	2.2
14	S	0.314	1.7	−0.20	N	1	0.25

[a] Atomic charges are values which approximate those found in the standard 20 amino acids in the commercially disributed version of the CHARMm force field.[2,14] The VDM E_{min} parameters and the atomic radius were from TRIPOS force field.[15] [b] A: acceptor, D: donor, B: both acceptor and donor, N: neither acceptor nor donor. When two atoms can hydrogen bond, their VDW interaction will be scaled to be softer by a factor of 0.7.

provide a better simulation of the real receptor. In contrast, a closed model is sensitive to redundant noise information that may hurt the predictive ability of the model and may be too tight for the new ligands to dock into. It is also important that in an open receptor model the key interactions will be more likely to stand out so that the model may rationally correspond to pharmacophore models and can be easier to analyze. Moreover, an Improved Genetic Algorithm (IGA) was used in FLARM to improve the computational performance. Several QSAR studies undertaken by using FLARM 1.0 gave good results.[9−12] In this paper, we will present the new FLARM 2.0 method which takes the flexibility of the ligand into account. In the process of receptor construction, the ligand in a FLARM 2.0 receptor model is now allowed to move its pose, that is, to change its conformation, orientation, and placement, through a minimization process till the lowest docking energy is achieved. The feature of flexible ligands together with the feature of flexible receptors that is already implemented in FLARM 1.0 make the FLARM 2.0 docking processes mimick the real binding processes to some extent.

FLARM 2.0 was proved to improve the quality of 3D-QSAR by producing more reasonable conformations and alignments. The results of our case studies show that the receptor models produced by FLARM 2.0 not only have high predictive ability but also correspond well with the pharmacophore models and/or the real receptors.

METHODS

Receptor Atom Types and the Initial Receptor Shape. The FLARM receptor models are constructed by 14 explicit atom types that are most likely to be encountered in the protein binding sites. We use these atom types to represent the key receptor atoms for receptor−ligand binding. Bond linking information between the atoms of the receptor model is ignored since it is unessential for the receptor−ligand interaction energy calculation. These 14 atom types together with their VDW interaction parameters (E_{min}), atomic radii, partial atomic charges, hydrogen bond (H-bond) properties, and occurrence weights are summarized in Table 1. The occurrence weights were approximated according to their occurrence rate in the natural binding sites calculated from a database of 200 protein−ligand complexes.[13] Note that there is an additional "void" atom type, i.e., no atom at all at a given spatial position, to allow for the possibility of open space on the receptor surface. GERM and PARM models also provide the void atom type but they do not intend to produce open receptor models, thus, the effect of their void atom type seems negligible − their receptor models are still "tightly closed" models. To obtain a real "open" model, we tried to increase the occurrence weight of void atom (to a chance of over 60%) in the atom selection procedure, and it turned out to be a simple and effective way to obtain open receptor models that allow for large gaps.

The initial shape of the receptor model, which is subject to the common surface of the superimposed training ligands, is generated by the following steps: (i) setting a total number of grid points and a cushion distance between receptor model and ligand; (ii) solving for the geometrical center of the superimposed training ligands, and with this point as the center, drawing a spherical surface with the least radius containing all ligand atoms, and then evenly producing a set of grid points on the spherical surface; and (iii) contracting each grid point to the spherical center along the radius by a step of 0.01 nm. Whenever the grid point bumps with any ligand atom, the contraction stops, and last the grid point expands a cushion distance along the radius. The initial receptor shape was then made after all the grid points were set. Obviously, like the conventional receptor model methods, this kind of initial receptor shape is determined by the conformations and the alignment of the training ligands. To avoid the bias of the initial coordinate setting, we introduced the flexible receptor concept. All the grid points (where receptor atoms were placed) in a FLARM receptor model are spatially moveable (in 0.1 nm range) in the process of genetic evolving. Thereby, cushion distance becomes an insensitive factor that does not affect much the computational results.

Binding Energy and Minimization. FLARM makes a basic assumption that if the ligands selected for study act on a common receptor target, the observed bioactivity is

proportional to the receptor−ligand binding free energy

$$\text{bioactivity} = a + b * \Delta G \quad (1)$$

where a and b are constants, and ΔG is the receptor−ligand binding free energy. This assumption was widely accepted in drug design studies especially when in vitro bioactivity data were used. The calculation of the receptor−ligand binding free energy is a complicated problem. There might be no universal energy function suitable for all drug systems in QSAR studies. Current scoring functions have standard errors of about 2 kcal/mol,[16] which is still too rough for QSAR studies. Hence, we make the assumption that the relative binding free energy can be approximated by the relative binding enthalpy energy since the various rotational, vibrational, and translational entropic and enthalpic contribution to binding should be approximately equal for analogues that bind to the same binding site. This assumption was used and proved to be acceptable by many QSAR studies. So, in the current FLARM version, the binding free energy remains simplified as the binding enthalpy energy that is calculated by molecular mechanics method using the TRIPOS 5.5 force field equations

$$E_{\text{vdw}} = \sum_{i=1}^{n}\sum_{j=1}^{m} E_{ij}(1.0/a_{ij}^{12} - 2.0/a_{ij}^{6}) \quad (2)$$

$$E_{\text{elec}} = 332.17 * \sum_{i=1}^{n}\sum_{j=1}^{m} q_i q_j/\epsilon_{ij} r_{ij} \quad (3)$$

$$\Delta G \sim E_{\text{bind}} = E_{\text{vdw}} + E_{\text{elec}} \quad (4)$$

where E_{elec} is the electrostatic energy, E_{vdw} is the steric energy, and E_{bind} is the total binding enthalpy energy. A detailed description of these energy terms can be found in the TRIPOS force field manual[15] or in ref 9.

In FLARM 2.0, the ligands inside the receptor models are subject to minimization before calculation of the binding energies. The ligands are considered flexibly moveable by the rotation of the rotational bonds inside the ligands and the rotation and translation of the ligands in three-dimensional space. A minimizer that uses the Powell algorithm, which is a nonderivative, local, and deterministic optimization algorithm, has been implemented in FLARM 2.0 for the binding energy optimization. During the optimization process, the ligand conformation is constrained by an internal energy limitation of 15.0 kJ/mol (user-adjustable value, and the internal energy is calculated by TRIPOS force field) above its initial internal energy. Note that since the Powell algorithm does not perform global minimization, the conformations of the ligands are not fully sampled. Though FLARM 2.0 considers both the flexibility of the ligand and the receptor model, the ligand and the receptor model do not move simultaneously: the receptor model is spacially and compositionally optimized in the process of genetic evolving but stays fixed throughout the ligand optimization process, and the conformations of the ligands are adjusted in response to receptor changes by the optimization process.

Receptor Model Evaluation. For QSAR researchers, overfitting is a serious problem which means that in the training set one can get a good correlation coefficient for the regression equation but obtain poor results for the predicting set. To reduce the chance of overfitting, like PARM and FLARM 1.0, we use the cross-validated R^2 (q^2) of the QSAR equation as the criterion to evaluate the quality of the FLARM 2.0 receptor models. In a leave-one-out cross-validation experiment involving n molecules for a given receptor model, a regression equation (in the form of eq 1) is built from all but the first molecule, and this equation is used to predict the activity of the first molecule. Then, all but the second molecule are used to create a regression equation that predicts the second molecule and so on. In this way, each molecule is predicted based on this receptor model, and the quality of the model is measured by q^2. q^2 is defined as

$$q^2 = 1 - \frac{\sum (a_i - p_i)^2}{\sum (a_i - \bar{a})^2} \quad (5)$$

where a_i are the experimental activities of the molecules, $\tilde{a}$ is the mean of the a_i, and p_i are the predicted molecular activities. The numerator is the squared errors of the predictions, and the denominator is a measure of how much variation there is in the actual activities.

Based on q^2, the final score of a receptor model is defined as

$$\text{score} = \begin{cases} q^2 - \text{average\_binding\_energy} * k & b < 0 \\ q^2 - \text{average\_binding\_energy} * k - 1.0 & b < 0 \end{cases} \quad (6)$$

where q^2 is as defined in eq 5. Average_binding_energy is a new term used by FLARM 2.0 that means the average binding energy of all the training ligands bound inside the receptor model. This term is used in the score function in order to reward low binding energy and to penalize high binding energy. k is a scaling factor with a default value of 0.0025 that can be modified by the users. b is the slope of the linear eq 1. A positive slope ($b >= 0$) is unacceptable since it means that higher binding energy leads to higher bioactivity. So, if any b is positive for a receptor model, its score will decrease by 1.0 as a severe penalty.

Genetic Algorithm. An improved genetic algorithm (GA) was used to obtain receptor models with high scores. In GAs, the solutions to the problem must be encoded in linear data structures called chromosomes. In FLARM 2.0, all receptor models are encoded with such chromosomes. Each chromosome consists of two parts. The first part is an integer string containing integers representing receptor atom type codes listed in Table 1. The second part is a real number string that stores the coordinates of the receptor atoms. To start the GA computation, a population (typically 100−200) of chromosomes must be initially generated. The initial shapes of the starting receptors are determined by the common surface of the training ligands and are set as described above (the initial shapes of all the individual receptors are the same), whereas the initial atom type assignment to the grid coordinates is random. We added a charge-complementary principle to initialize the receptor atom types. We believe this principle is reasonable and can speed up the genetic evolving process. For each grid point, first the charge of the closest atom of each ligand is summed up and then averaged to be q_0, and then an atom type is randomly assigned to this

point with the possibility weight p defined as

$$p = k*O*e^{\text{focus}*|q+q_0|} \quad (7)$$

where k and focus are constants, O is the occurrence weight of the receptor atom type that is listed in the last column of Table 1, and q is the partial atomic charge of the receptor atom type that is also listed in Table 1. The charge-complementary principle is only used in the initialization step. In the later process of genetic evolving, the probability of an atom type being selected is only linearly on its occurrence weight. In the process of genetic evolving, the coordinates of the receptor atoms are moveable within a 0.1 nm-radius range around their initial positions. As the average distance of two receptor atoms is about 0.2 nm, a moving radius of 0.1 nm is enough. The genetic evolving process ends on the condition that either the maximal number of iteration (generations) is reached or the highest score meets a preset criterion. The default maximal generation is 200, and the score criterion is case-dependent and its default value is 0.80. An excessive high score criterion such as 0.95 will greatly increase the chance of overfitting since the models may even have to fit the experimental errors and therefore is not recommended in FLARM (in fact, FLARM 2.0 seldom can create a very high score). When the genetic evolving process ends, the 15 receptor models with the highest scores will be output by FLARM. Usually the models are simple, concise, explicit, and manually analyzable and can be used to predict the activities of new ligands.

FLARM GA is a kind of generation-replacement nonduplicate GA and uses a special mutation technique to improve its performance. FLARM GA has three mutation operators: point mutation operator, segment mutation operator, and circular operator. The latter two mutation operators can cause large mutations that help keep the population diverse. Moreover, the crossover operator of FLARM uses a special strategy such that chromosomes with similar score are more likely to mate, which we believe can accelerate the evolving speed.

Message Passing Interface (MPI) Parallel Computation. In FLARM 2.0, the computational time of a score function with an embedded energy optimization process will be hundreds or thousands of times longer than that of a score function without an energy optimization process. That is, the FLARM 2.0 computation always turns out to be extremely time-consuming and is beyond the computational ability of a single CPU. To solve this problem, we have implemented the FLARM 2.0 parallel computation by using a Message Passing Interface (MPI). Briefly, the workflow of FLARM 2.0 parallel computation is as follows: the primary computational node evenly distributes the computational tasks for calculating the scores for the whole population to different computational nodes; after all distributed computation jobs are finished, all scores are collected together and then broadcasted to all nodes by the primary node; after the very quick step of genetic evolving to generate the next population that is run simultaneously by all the nodes, the primary node again distributes the computational tasks for calculating the scores to all the nodes as it does in the first step, and then this loop continues. Since GA is a kind of stochastic algorithm, it is necessary to make sure that all the nodes use the same random numbers to obtain identical computational results. By using parallel computation, the computational time of our three flexible-ligand case studies varies from about 1 to 30 h on a SUNWAY cluster using 50 Intel CPUs of 2.4 GHz.

Programming and Availability. The computer programs FLARM 1.0 and FLARM 2.0, written in ANSI C++, read the aligned training molecules (represented in SYBYL/Mol2 format) as well as their bioactivity data and then construct pseudoreceptor models via genetic algorithms. Users can then use the FLARM receptor models to predict the bioactivities of new ligands. FLARM has a few adjustable parameters included in a parameter file. Users can choose to either use the default values or to set their own values. FLARM 1.0 has DOS, Windows, and Linux versions, but FLARM 2.0 only has a Linux version. FLARM 2.0 shares the same functions as FLARM 1.0 except that it has an additional flexible-ligand running mode. All programs can be downloaded at ftp://mdl.ipc.pku.edu.cn/pub/softwares/FLARM2.

RESULTS AND DISCUSSION

We have applied FLARM 2.0, i.e., the flexible-ligand mode FLARM to perform QSAR analyses on three drug systems. The first system is 31 corticosteroid binding globulin(CBG)-binding steroids that were studied in Cramer's original CoMFA paper.[17] The second system is 29 rat γ-aminobutyric acid (GABA) receptor inhibitors that were previously studied by using CoMFA and FLARM 1.0 methods.[12] The third system is 50 cyclooxygenase-2 (COX-2) inhibitors that were previously studied by Liu et al.[18] using the CoMFA method with a receptor-based alignment. These three case studies were carried out as not only validations of the FLARM 2.0 methodology but also as independent QSAR studies for their own drug design usage.

Steroids. We applied FLARM 2.0 to the steroid's CBG binding affinity prediction problem. The standard data set (shown in Figures 1 and 2) contained 31 steroids which Cramer et al. used to develop CoMFA.[17] The first 21 molecules were used as the training set, and the remaining 10 molecules were included in the predicting set. The molecular models of the 21 steroids in the training set were already modeled and were supplemented by SYBYL.[15] Therefore we extracted the prealigned structures of the training molecules directly from the SYBYL 6.91 package. Since the molecular models of the 10 steroids in the predicting set were not provided by SYBYL, they were constructed manually according to their closest structures in the training set, respectively. The new modified part of each predicting molecule was partly minimized by using the TRIPOS force field.[15] Partial atomic charges were calculated by the method of Gasteiger and Marsili, as were done in the original CoMFA study. The models of the 10 steroids in the predicting set were not constructed exactly the same way as the training steroids. The training steroids were constructed starting with coordinates taken from the Cambridge Crystallographic Database, minimizing using the standard Tripos force field, searching the side chain torsional space on a 10-degree grid, and minimizing the final structure again.[17] Nonetheless, since in FLARM 2.0 the conformations and the alignments are not very critical for the results, we intended to use FLARM 2.0 to analyze the data set and to predict the somewhat inaccurate (constructed not fully

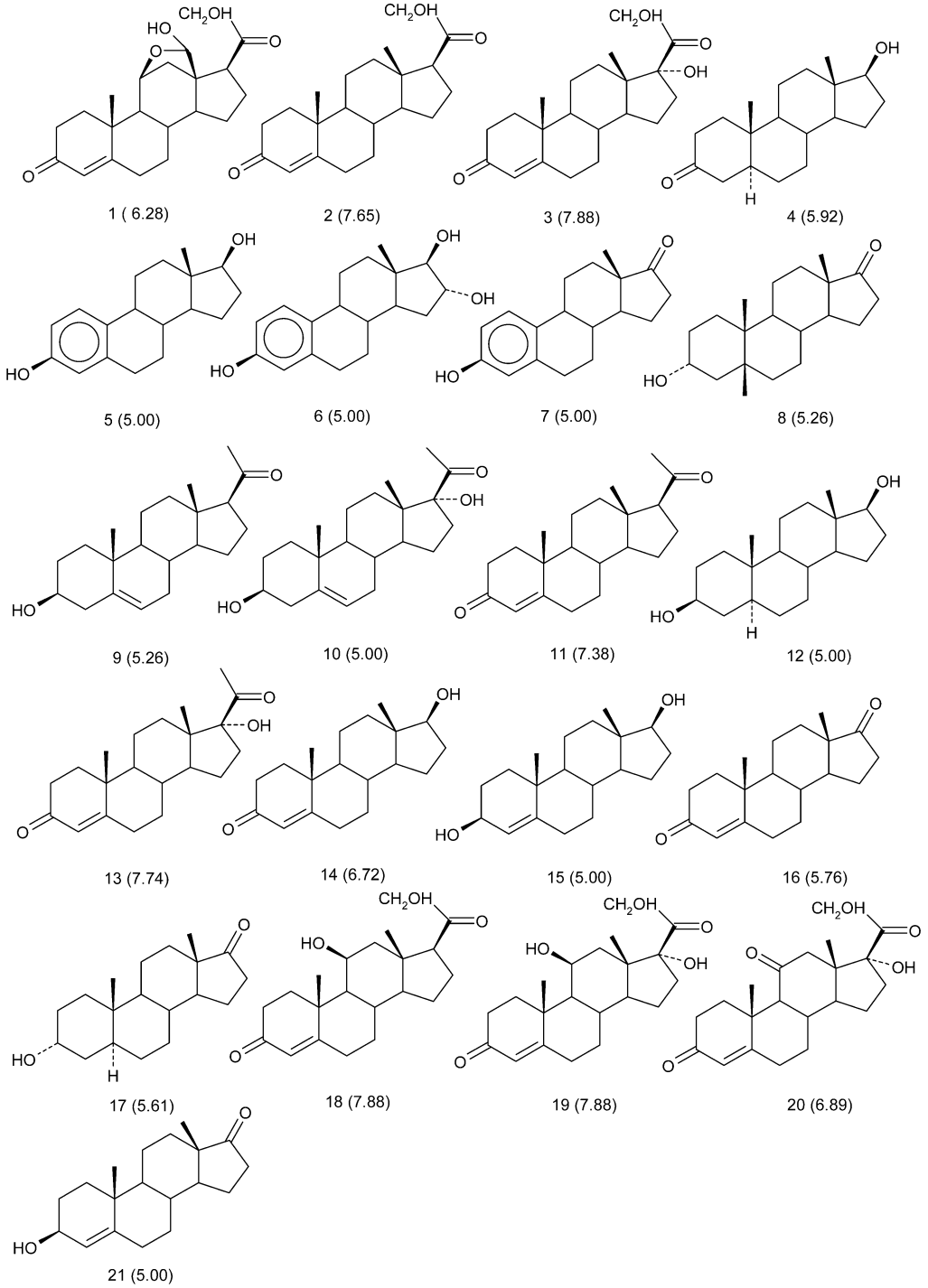

Figure 1. Structures and CBG binding affinities of steroids in the training set.

consistently with the training set) structures in the predicting set. The FLARM 2.0 computation settings were as follows: receptor atom number = 45 (with about 20−25 void atoms), maximum genetic generations = 150, population size = 110, q^2 terminal condition = 0.80, and maximum Powell minimization iterations = 2000. After the training run, FLARM 2.0 yielded 15 receptor models that have high conventional correlation coefficients and q^2. The predictive results of the FLARM 2.0 receptor model 8 (this model has the lowest predictive standard deviation) as well as the predictive results reported by CoMFA studies[17] and by CoMSIA studies[19] are listed and compared in Table 2. For the training set of 21 molecules, the computational results of the FLARM 2.0 model are $r^2 = 0.854$, sd = 0.459, and $q^2 = 0.852$. For the test set, we use the correlation coefficient and the predictive standard deviation (S_{pred}) to evaluate the quality of prediction

$$S_{pred} = \sqrt{\sum(\text{activity, predicted} - \text{activity, experimental})^2/N} \quad (8)$$

where N is the number of the predicted molecules. The model successfully predicted the predicting set with a correlation coefficient of 0.598 and a S_{pred} of 0.655, which are both better than those of CoMFA reported by Cramer et al.[17] and those of CoMSIA reported by Klebe et al.[19] Figure 3 shows the correlation between the FLARM 2.0 predicted activities and the experimental activities for all the steroids. For the whole

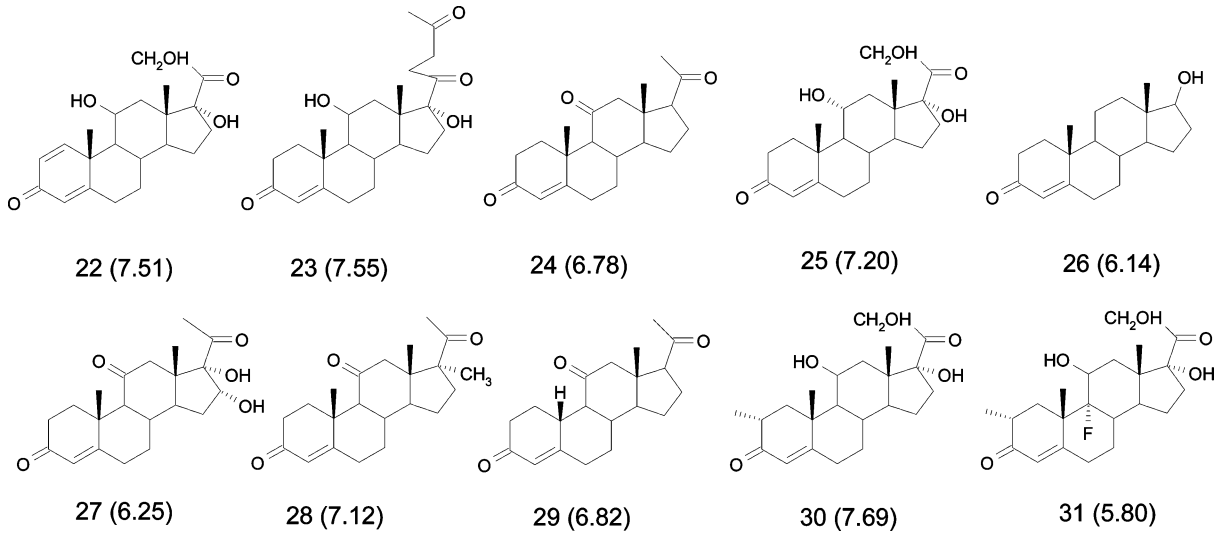

Figure 2. Structures and CBG binding affinities of steroids in the test set.

Table 2. Computation Results of Steroids[a]

molecule	CBG	FLARM 2.0 predicted	FLARM 2.0 residue	FLARM E_{bind} (kcal/mol)	CoMFA predicted[b]	CoMFA residue	CoMSIA predicted[c]	CoMSIA residue
22	7.51	8.16	−0.65	−19.31	6.54	0.97	7.62	−0.11
23	7.55	8.10	−0.55	−19.11	7.54	0.01	7.68	−0.13
24	6.78	7.00	−0.22	−15.47	6.53	0.25	6.52	0.26
25	7.20	8.01	−0.81	−18.81	7.55	−0.35	7.75	−0.55
26	6.11	5.97	0.14	−12.09	5.96	0.15	5.81	0.30
27	6.25	6.50	−0.25	−13.84	7.06	−0.81	7.18	−0.93
28	7.12	6.44	0.68	−13.65	5.38	1.74	7.35	−0.23
29	6.82	6.62	0.20	−14.22	7.01	−0.19	6.9	−0.08
30	7.69	7.18	0.51	−16.07	7.23	0.46	7.66	0.03
31	5.80	7.22	−1.42	−16.21	6.94	−1.14	7.82	−2.02
			$r = 0.598$, $S_{pred} = 0.655$		$r = 0.229$, $S_{pred} = 0.799$		$r = 0.437$, $S_{pred} = 0.741$	

[a] The FLARM 2.0 computational results for the training set of 21 molecules are $r^2 = 0.854$, sd = 0.459 and $q^2 = 0.852$, and the activity-energy linear function is as follows: activity (CBG) = 2.248 + (−0.305) * E_{bind}. [b] Data cited from ref 17. [c] Data cited from ref 19. The alignment is based on mutual similarity indices pairwise calculated between all atoms of the molecules being compared, according to a modified version of the program SEAL.[20]

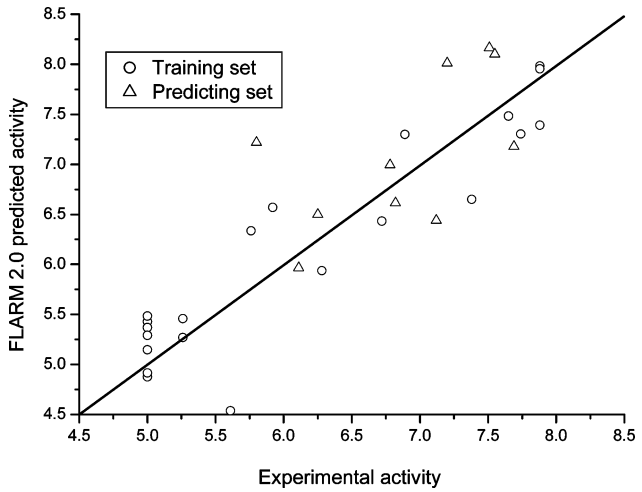

Figure 3. Scatter plots of the FLARM 2.0 predicted activities versus the experimental activities for the 31 steroids.

set of 31 molecules, the statistical results of FLARM 2.0 prediction are r^2 =0.782 and sd = 0.514. Here, the FLARM 2.0 receptor models were proved more robust than CoMFA in performing prediction as we expected, because the binding energy minimization procedure makes the prediction more feasible and stable. We think this is an important improvement as it relieves the uncertainty of 3D-QSAR results caused by conformation and the alignment problems. Though FLARM 2.0 is designed to be tolerant of conformation and alignment deviation, the initial conformation and alignment of the molecules should still be carefully chosen. Variations within limited range can be recovered; however, FLARM 2.0 will fail to predict the results when the deviation is large. We have tried to change the poses of molecule **22** by rotating one of its rotatable bonds or rotating one of the axes in 3D space by 15 degrees. FLARM 2.0 recovered all the variations to near-original predictions (all deviations are less than 0.3). But when the rotations reached 30 degrees, FLARM 2.0 failed to recover some of the variations and get unacceptable predictions (some deviations are greater than 1.0).

As the poses of the ligands after minimization were not the same as their starting poses, it is interesting to analyze the final optimized conformations and alignment of the ligands. The final conformations and alignment of the 21 training steroids inside receptor model 8 are shown in Figure 4b; their starting conformations and alignments (by a rigid-body least-squares fitting rule) prepared by Crammer et al. are shown in Figure 4a. It can be seen that after the FLARM 2.0 computation, the conformations of the steroids changed, and the final alignment was not so orderly as the starting alignment. Instead, the final alignment is like some receptor-based alignment derived from crystal structures or docking

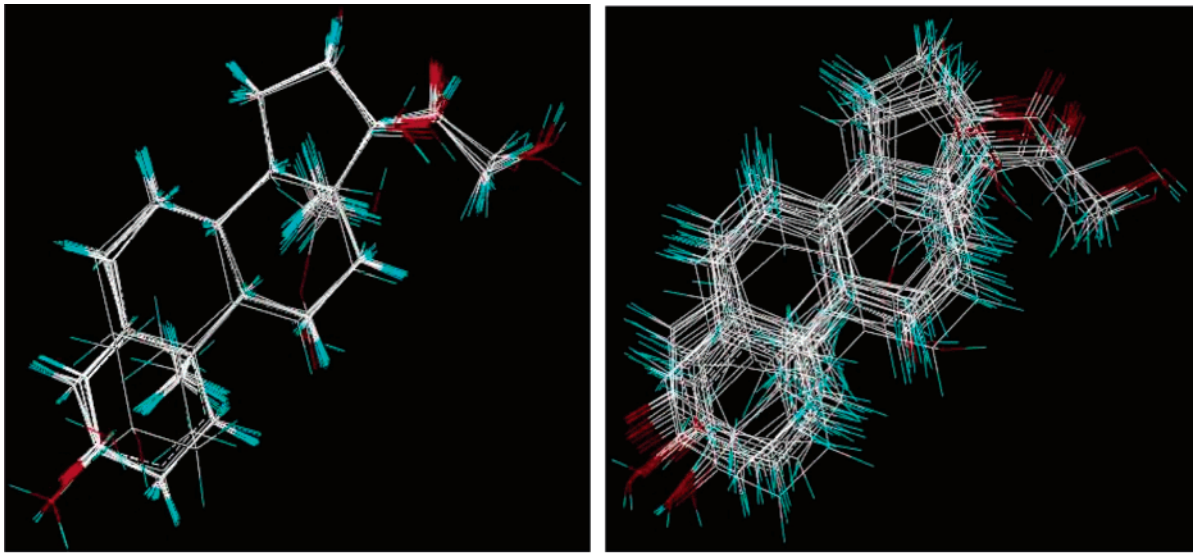

(a) (b)

Figure 4. (a) The starting conformations and alignment of the training steroids. (b) The final conformations and alignment of the training steroids.

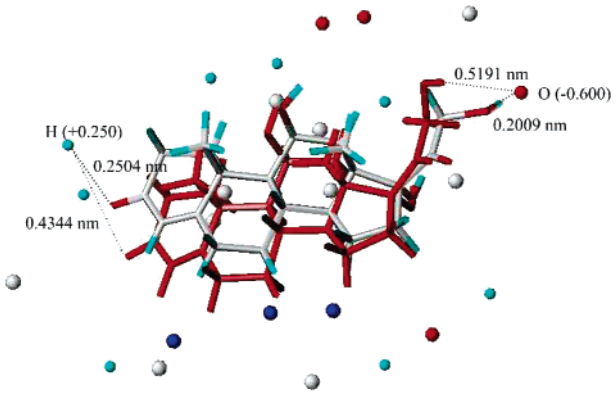

Figure 5. The starting pose (colored in red) and the final optimized pose (colored by atom types) of molecule **19** inside the FLARM receptor model (colored by atom types). There are two hydrogen bonds formed between the receptor model and the final pose of molecule **19**. They are marked with dashed lines and distance values. The starting geometries of the hydrogen bonds and their distances are also marked.

studies. These results show that FLARM 2.0, without using any receptor information, produced receptor-based-like conformations and alignments for the ligands and practically improved the quality of the 3D-QSAR models.

In Figure 5 we illustrated the starting pose and the final optimized pose of molecule **19** inside the FLARM 2.0 receptor model. It can be seen that there exist two hydrogen bonds that are important for the final binding: in the left, a carbonyl oxygen of the molecule forms a hydrogen bond with a charged hydrogen atom of the receptor model with a distance of 2.50 Å; in the right, a hydroxyl hydrogen of the molecule forms a hydrogen bond with a hydroxyl oxygen atom of the receptor model with a distance of 2.01 Å. However, for the starting pose of the molecule, such hydrogen bonding cannot be formed since the distances of the donor and the acceptor atoms are 4.34 and 5.19 Å, respectively. The formation of the two hydrogen bonds is the result of the flexible optimization of the molecule inside the receptor model.

Rat GABA Receptor Inhibitors. GABA plays an important role as a major inhibitory neurotransmitter in both vertebrates and invertebrates, which have similar but pharmacologically distinct GABA receptors.[21] The structures of the 29 inhibitors reported by Ozoe's group[21−23] are displayed in Figure 6, and their rat GABA receptor inhibitive activities are displayed in Table 3. These inhibitors were already studied by using CoMFA and FLARM 1.0.[24,12] In the CoMFA and FLARM 1.0 studies, the molecular models of the inhibitors were built with SYBYL 6.91. Molecule **14** was selected as the starting structure, and its starting geometry was taken from the low-energy conformation created by a RANDOMSEARCH procedure embedded in SYBYL. Then it was used as a template to construct other molecules by modifying and assembling fragments from the SYBYL standard library. All the molecular models were finally minimized again with Tripos force field, and the partial atomic charges were calculated by a semiempirical AM1 method using the MOPAC module embedded in SYBYL. All molecules were aligned according to the least-squares fitting of the six benzene carbon atoms and the two opposite atoms connecting the two biggest groups to the benzene. After the above preparations, CoMFA and FLARM 1.0 analyses were performed. Good results were obtained for the fly GABA receptor inhibitory activities (The CoMFA q^2 is 0.679, and the FLARM 1.0 q^2 is 0.874 with a S_{pred} of 0.287 for 6 independent predicting molecules); however, only after the deletion of molecules **1**, **8**, **15**, **19**, **B10_2**, **C18**, and **C25** were the results for the rat GABA receptor inhibitory activity acceptable.[12,24] That is, the conformers and alignment of the inhibitors used seem proper for the fly GABA receptor but are less accurate for the rat GABA receptor. We believe several reasons may exist: (1) different receptors may cause different binding poses of ligands; (2) the ligands used here have three different kinds of skeleton structures; and (3) these inhibitor were designed to inhibit the invertebrate GABA receptors and their inhibitive activities for the rat GABA receptor (namely toxicity) are 1−2 magnitudes lower and their binding may be less specific.

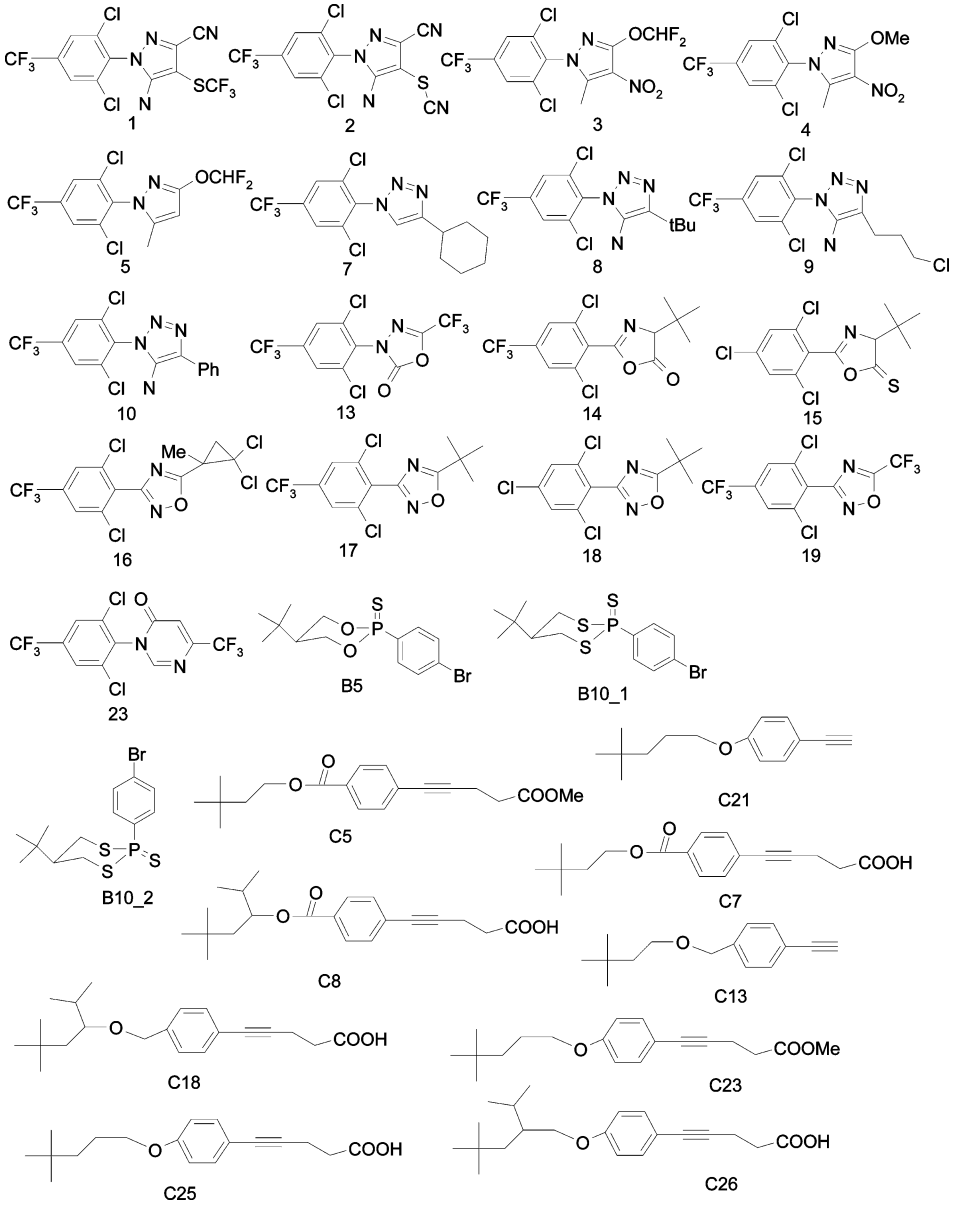

Figure 6. Structures of the rat GABA receptor inhibitors.

Table 3. Experimental and FLARM Predicted Activities of the GABA Receptor Inhibitors

molecule	pIC_{50}	FLARM 2.0 predicte[a]	molecule	pIC_{50}	FLARM 2.0 predicted	molecule	pIC_{50}	FLARM 2.0 predicted
1	6.75	6.79	**14**	6.62	5.92	**C5**	6.66	6.64
2	5.02	5.32	**15***	5.60	5.85	**C7**	7.06	6.93
3*	6.73	6.03	**16**	6.35	5.77	**C8**	5.85	5.88
4	4.98	5.18	**17***	6.24	5.89	**C13**	5.47	5.76
5	5.00	5.72	**18**	5.67	5.61	**C18***	5.26	6.10
7	5.18	5.61	**19***	6.54	5.47	**C21**	5.29	5.46
8	6.34	5.48	**23**	5.83	5.81	**C23**	6.89	6.17
9	5.75	6.02	**B5**	7.40	7.40	**C25***	7.00	6.45
10	5.96	5.86	**B10_1**	6.92	7.28	**C26**	5.54	5.93
13*	5.32	5.55	**B10_2***	5.97	6.36			

[a] The FLARM 2.0 predicted values are calculated from the FLARM 2.0 model 1. The FLARM 2.0 computational results for the training set of 21 molecules are $r^2 = 0.693$, sd = 0.426, and $q^2 = 0.656$, and for the test set of 8 molecules are $r = 0.292$ and $S_{pred} = 0.616$. The activity-energy linear function is $pIC_{50} = 4.577 + (-0.242) * E_{bind}$.

In this paper we used FLARM 2.0 to reanalyze the inhibitory activity of the 29 inhibitors against rat GABA receptor. We expect that with the optimization process of ligands implemented by FLARM 2.0, the 7 above molecules are not required to be deleted from the data set. In this study, we checked all the 29 molecules and selected the molecules **3**, **13**, **15**, **17**, **19**, **B10_2**, **C18**, and **C25** as the predicting set and the remaining 21 molecules as the training set. The predicting set was selected to cover a wide range of activity and chemical diversity. The computation settings were as

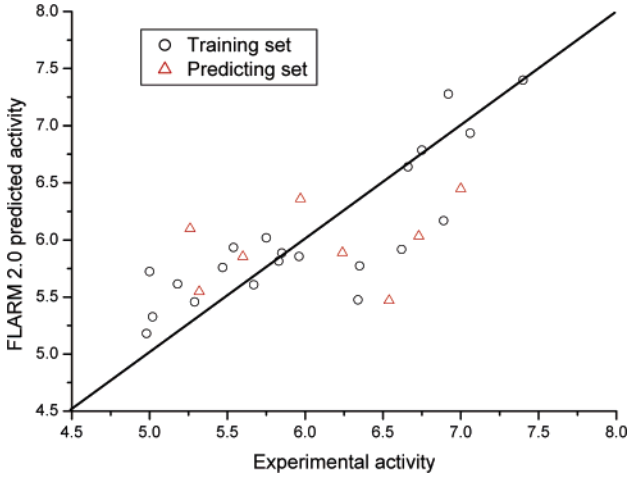

Figure 7. The scatter plots of the FLARM 2.0 predicted activities versus the experimental activities for the GABA receptor inhibitors.

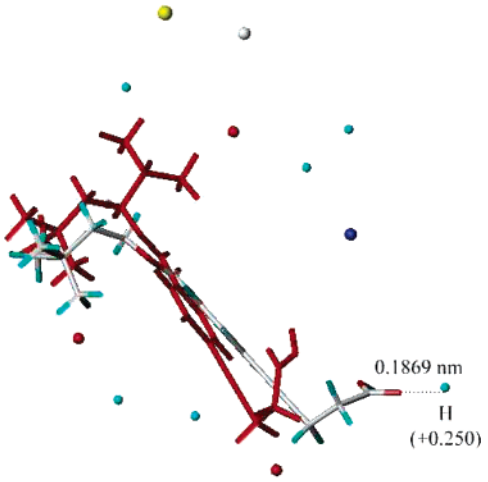

Figure 8. The final optimized pose of **C7** (colored by atom types) and **C8** (colored in red) inside the FLARM receptor model (colored by atom types). There is an important hydrogen bond formed between the receptor model and **C7**. However, due to the steric influence of the additional isopropyl group, **C8** adopts an orientation that is a little bit different from that of **C7** and the hydrogen bonding cannot be formed.

follows: receptor atom number = 45, maximum genetic generations = 150, population size = 110, q^2 terminal condition = 0.80, and maximum Powell minimization iterations = 1000. After the training run, FLARM 2.0 yielded 15 receptor models, and the first model has the lowest predictive standard errors for both the training set and the test set. The computational results of the first receptor model are listed in Table 3. For the training set of 21 molecules, the computational results of the model are $r^2 = 0.693$, sd = 0.354, and $q^2 = 0.656$. The model predicted the test set with a correlation coefficient of 0.292 and a S_{pred} of 0.616. The main prediction error is from **19** and **C18**, and if they are omitted, the prediction results are $r = 0.719$ and $S_{pred} = 0.444$. Of the 7 molecules **1**, **8**, **15**, **19**, **B10_2**, **C18**, and **C25** that previously could not be correctly calculated by the CoMFA and FLARM 1.0 methods, the predicted results for **1**,**15**, **B10_2**, and **C25** are now acceptable, though the predicted results for **8**, **19**, and **C18** are still somewhat disputable. Figure 7 shows the correlation between the FLARM 2.0 predicted activities and the experimental activities for all 29 molecules. For the whole set of 29 molecules, the statistical results of prediction are $r^2 = 0.549$ and sd = 0.381.

In Figure 8 we illustrated the final optimized pose of **C7** (colored by atom types) and **C8** (colored in red) inside the FLARM receptor model (colored by atom types). There is a hydrogen bond (bond length 1.87 Å) formed between the receptor model and **C7**. However, due to the steric influence of the additional isopropyl group, **C8** adopts an orientation that is a little bit different from that of **C7** and the hydrogen bond cannot be formed. This hydrogen bond is very important for rat GABA receptor inhibition, and that is why **C7** has a higher inhibitory activity while **C8** has a lower inhibitory activity. In the FLARM 2.0 receptor model for fly GABA receptor (results not presented in this paper), this hydrogen bond does not exist at all. So we can infer that in order to design a molecule with high pesticidal activity and low toxicity to vertebrates, this hydrogen bonding should be avoided.

We note that molecule **19** is very similar to molecule **13**, which has a low pIC_{50} of 5.32, and only these two molecules have a distinct CF_3 group that does not exist in other molecules. This may be the reason that FLARM 2.0 underestimates the activity of **19** as CoMFA and FLARM 1.0 do, as FLARM 2.0 is not designed to have the ability to avoid this kind of error. And maybe for a similar reason molecule **8** is also underestimated. For molecule **C18**, the experimental pIC_{50} is 5.26 and the predicted pIC_{50} is 6.10. The activity of **C18** is overestimated since its skeleton structure is a little bit different from **C8** and FLARM 2.0 can just barely change the pose of **C18** to form the hydrogen-bonding mentioned above.

COX-2 Inhibitors. In 2002, Liu et al. studied 50 cyclooxygenase-2 (COX-2) inhibitors (listed in Table 4) employing combined computational methods of automated molecular docking with 3D-QSAR approaches.[18] They first used AUTODOCK 3.0[25] to dock all the molecules to the binding site of COX-2 and then used the binding conformations and their alignments at the binding site to perform CoMFA and CoMSIA studies. The resulted q^2 values were 0.635 and 0.641 for CoMFA and CoMSIA models, respectively. Here we use FLARM 2.0 to analyze these 50 1,5-diarylpyrazole molecules as a case study in order to compare FLARM 2.0 to receptor-based 3D-QSAR methods. Just as in Liu et al.'s work, the first 40 (**3**−**42**) molecules were used as the training set and the last 10 (**1***−**10***) were used as the predicting set. Molecule **3** was selected as the template molecule. The lowest-energy conformation of **3** was determined by using a SYSYTEMATIC search procedure with a 10-degree step size for all the rotational bonds and a final Powell optimization procedure embedded in SYBYL. It was found that the lowest-energy conformation of molecule **3** is nearly the same as the X-ray structure of **SC-558** (also listed in Table 4) bound to COX-2 (PDB code 1CX2), but their sulfonamide moieties adopt nearly opposite orientations. However, we still chose to use the lowest-energy conformation of **3** in order to do a blind experiment as if we had no experimental structure information. All the other molecule models were constructed based on the lowest-energy conformation of **3** by modifying and assembling fragments from the SYBYL standard library. The orientations of the subgroups of all the molecules were attentively kept consistent

Table 4. Structures of 1,5-Diarylpyrazole Molecules and Their Inhibitory Activities

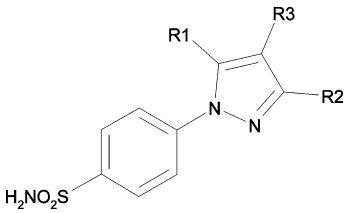

compd	R_1	R_2	R_3	pIC_{50}
3	phenyl	CF_3	H	7.50
4	2-F-phenyl	CF_3	H	7.24
5	4-F-phenyl	CF_3	H	7.39
6	2-Cl-phenyl	CF_3	H	7.25
7	2-Me-phenyl	CF_3	H	7.16
8	4-Me-phenyl	CF_3	H	7.40
9	4-CN-phenyl	CHF_2	H	4.53
10	4-COOH-phenyl	CHF_2	H	4.33
11	4-NO_2-phenyl	CF_3	H	5.58
12	4-SMe-phenyl	CF_3	H	8.05
13	2-NMe_2-phenyl	CF_3	H	4.84
14	4-NHMe-phenyl	CF_3	H	7.80
15	4-CH_2OH-phenyl	CF_3	H	4.03
16	4-COOH-phenyl	CF_3	H	4.95
17	3-chloro-4-methoxyphenyl	CHF_2	H	7.57
18	3-methyl-4-methoxyphenyl	CF_3	H	8.03
19	3-methyl-4-(methylthio)phenyl	CF_3	H	8.43
20	3-fluoro-4-(dimethylamino)phenyl	CF_3	H	8.24
21	3-chloro-4-(methylamino)phenyl	CF_3	H	7.57
22	3,5-dichloro-4-methoxyphenyl	CHF_2	H	7.68
23	3,5-difluoro-4-methoxphenyl	CHF_2	H	6.46
24	3,4-dichlorophenyl	CF_3	H	7.82
25	2,4-dimethylphenyl	CF_3	H	6.92
26	2-pyridyl	CF_3	H	4.34
27	3-pyridyl	CF_3	H	4.35
28	4-pyridyl	CF_3	H	4.19
29	5-chloro-2-thienyl	CF_3	H	7.59
30	5-(2,3−2H-benzofuran)	CF_3	H	7.68
31	phenyl	CH_3	H	4.20
32	4-Cl-phenyl	CF_3	Cl	8.28
33	4-Cl-phenyl	CF_3	Me	7.66
34	4-Cl-phenyl	CF_3	Et	7.55
35	phenyl	CF_3	OMe	7.10
36	phenyl	H	CH_3	4.33
37	4-CH_3-phenyl	H	CN	7.12
38	4-Cl-phenyl	H	SO_2Me	4.70
39	phenyl	H	NH_2	4.53
40	4-Cl-phenyl	CN	Cl	8.00
41	4-Cl-phenyl	COOMe	Cl	6.80
42	4-Cl-phenyl	$CONH_2$	Cl	5.96
1* [a]	4-Cl-phenyl	CF_3	H	8.00
2* [a]	3-Me-phenyl	CF_3	H	6.96
3* [a]	2-OMe-phenyl	CF_3	H	6.54
4* [a]	4-OMe-phenyl	CF_3	H	8.10
5* [a]	3,4-dimethoxyphenyl	CF_3	H	6.22
6* [a]	5-methyl-2-furyl	CHF_2	H	5.48
7* [a]	1-cyclohexenyl	CF_3	H	7.08
8* [a]	phenyl	CHF_2	H	6.89
9* [a]	4-Cl-phenyl	CH_2OCH_2Ph	H	7.54
10* [a]	4-F-phenyl	CN	H	6.47
(SC-558)	4-Br-phenyl	CF_3	H	8.89

[a] Molecules in the predicting set.

to their corresponding subgroups of **3**. All the molecular models were finally minimized with Tripos force field and were aligned according to the least-squares fitting of the two common rings. All atoms were assigned Gasteiger−Hückel charges as were done by Liu et al.

After the above preparations, FLARM 2.0 analyses were performed. The FLARM 2.0 computation settings were as follows: receptor atom number = 59, maximum genetic generations = 200, population size = 110, q^2 terminal condition = 0.70, and maximum Powell minimization iterations = 2000. After the training run, FLARM 2.0 yielded 15 receptor models, and the first model had the lowest predictive standard errors for both the training set and the test set. The computational results of the first receptor model are listed in Table 3. For the training set of the 40 molecules, the computational results of the model are $r^2 = 0.600$, sd = 0.741, and $q^2 = 0.610$. The model predicted the 10 test molecules with a correlation coefficient of 0.583 and a S_{pred} of 0.986. The main prediction error is from **8*** and **9***, and if these outliers are omitted, the prediction results increase to $r = 0.729$ and $S_{pred} = 0.731$. The starting and the final conformations and alignments of all the 50 molecules were shown in Figure 9. It can be seen that after the FLARM 2.0 computation, the conformations of the molecules changed, and the final alignments were not so orderly as the starting alignment. The final alignment is similar to the receptor-based alignment reported by Liu et al.[18] and Datar et al.[26] and proves again that FLARM 2.0, without using any receptor information, produces receptor-based-like conformations and alignments for the ligands.

CoMFA and FLARM 1.0 computations were also carried out as comparisons. In doing the CoMFA computations, default parameters were used. For the original conformations and alignments (CoMFA 1), the CoMFA training results are $q^2 = 0.212$, component (n) = 1, conventional $r^2 = 0.411$, and sd = 1.161, and the predicting results are $r = 0.342$ and $S_{pred} = 0.986$. For the conformations and alignments after FLARM 2.0 computation (CoMFA 2), the CoMFA training results are $q^2 = 0.408$, component (n) = 1, conventional $r^2 = 0.600$, and sd = 0.957, and the predicting results are $r = 0.674$ and $S_{pred} = 0.822$. FLARM 2.0 performs better than CoMFA 1 for both the training and the predicting set, and it is also clear that the conformations and alignments produced by FLARM 2.0 is significantly better than the original ones for CoMFA studies. In doing the FLARM 1.0 computations, the parameters were the same as those of FLARM 2.0 except that the flexible ligand mode was off. The predictive results for **9*** were not very stable since its large R_2 group (which is odd since all the R_2 groups in the training set are much smaller than that of **9***) often collides with the receptor models. We selected a model that did not collide severely with **9*** and the results are as follows: for the training set, $q^2 = 0.711$, $r^2 = 0.710$, and sd = 0.687 and for the predicting set, $r = 0.343$ and $S_{pred} = 1.090$. Though the training results of FLARM 1.0 are better than those of FLARM 2.0, the predicting results of FLARM 2.0 are better than those of FLARM 1.0, which means that FLARM 2.0 does not tend to overfit and is more robust for prediction. All the above computational results are summarized and compared in Table 5.

Figure 10 shows the correlation between the FLARM 2.0 predicted activities and the experimental activities. For the whole set of 50 molecules, the statistical results are $r^2 = 0.539$ and sd = 0.778. Liu et al.[18] reported that the correlation coefficient of the experimental activities and the AUTODOCK 3.0 predicted binding free energy for the 40 training molecules is 0.648.[18] Since FLARM 2.0 predicted activity is linearly dependent on the FLARM 2.0 receptor−ligand binding energy, Figure 10 actually shows the correlation between the experimental activities and the FLARM

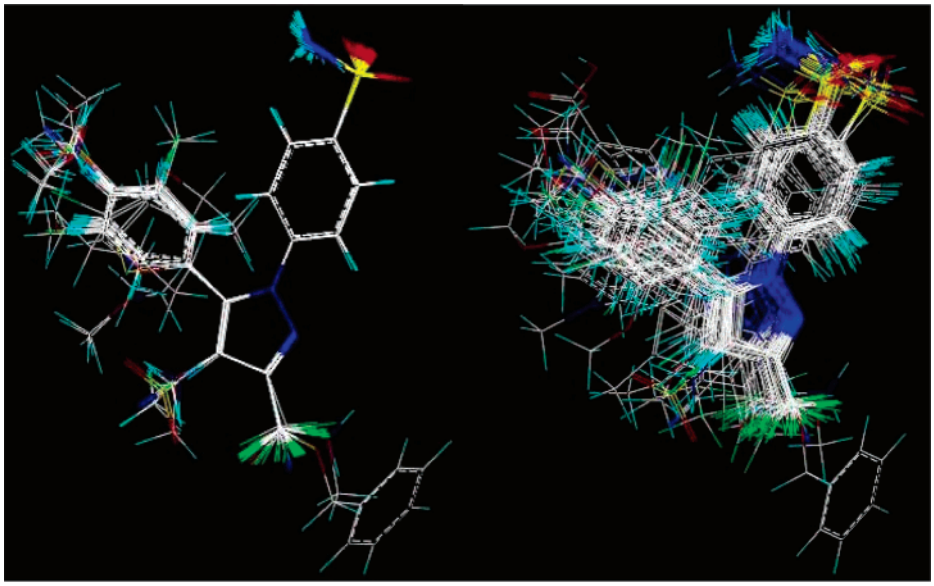

(a) (b)

Figure 9. (a) The original conformations and alignment of the COX-2 inhibitors. (b) The final conformations and alignment of the COX-2 inhibitors produced by FLARM 2.0.

Table 5. Computation Results for the COX-2 Inhibitors

molecule	pIC_{50}	FLARM 2.0 predicted	FLARM 1.0 predicted	CoMFA 1 predicted[a]	CoMFA 2 predicted[a]
1*	8.00	6.77	7.18	7.03	7.37
2*	6.96	7.53	6.51	6.90	7.94
3*	6.54	7.59	5.61	6.65	7.12
4*	8.10	7.79	6.09	6.99	7.49
5*	6.22	6.03	5.52	6.89	5.52
6*	5.48	4.66	5.87	5.59	4.96
7*	7.08	7.21	7.92	6.90	6.67
8*	6.89	5.07	6.68	5.28	6.58
9*	7.54	6.08	5.38	5.45	5.84
10*	6.47	5.75	6.68	6.20	5.59
predicting results		$r = 0.583$	$r = 0.343$	$r = 0.342$	$r = 0.674$
		$S_{pred} = 0.986$	$S_{pred} = 1.090$	$S_{pred} = 0.986$	$S_{pred} = 0.822$
training results[b]		$q^2 = 0.600$	$q^2 = 0.711$	$q^2 = 0.212$	$q^2 = 0.408$
		$r^2 = 0.610$	$r^2 = 0.710$	$r^2 = 0.411$	$r^2 = 0.600$
		sd = 0.740	sd = 0.687	sd = 1.161	sd = 0.957

[a] CoMFA 1: original conformations and alignments were used; CoMFA 2: the conformations and alignments produced by FLARM 2.0 were used. [b] Detailed computational results for the training set are not listed.

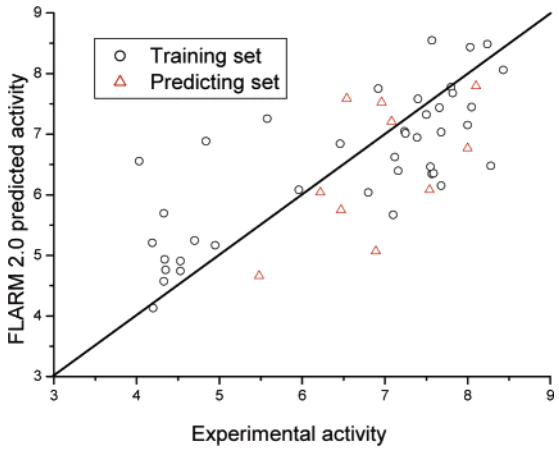

Figure 10. The scatter plots of the FLARM 2.0 predicted activities versus the experimental activities for the 50 COX-2 inhibitors.

2.0 predicted binding free energy. For the 40 training molecules, the correlation coefficient r^2 is 0.600, which is close to the activity-AUTODOCK binding free energy correlation coefficient r^2 . It is worth mentioning that the AUTODOCK binding free energies were calculated from the real protein structure, while the FLARM binding energies were calculated from just the pseudoreceptor model. This interesting comparison proves the validity of the FLARM 2.0 receptor models.

In the previous FLARM 1.0 studies, the FLARM 1.0 models were proved to correspond well with the pharmacophore models and/or the binding sites of the real protein receptors.[9−11] Since the 3D structures of COX-2 are available, we can compare the FLARM 2.0 receptor model to the real substrate-binding site of COX-2. Figure 11a displays the final binding mode of **5** (the molecule most-similar to **SSC-558**) inside the FLARM 2.0 model. Figure 11b displays the binding mode of **SSC-558** inside the binding site of COX-2 (PDB code 1CX2). In Figure 11b only the residues that contribute to the binding (calculated by SCORE[27−29]) are displayed for clarity. We have drawn four additional circles

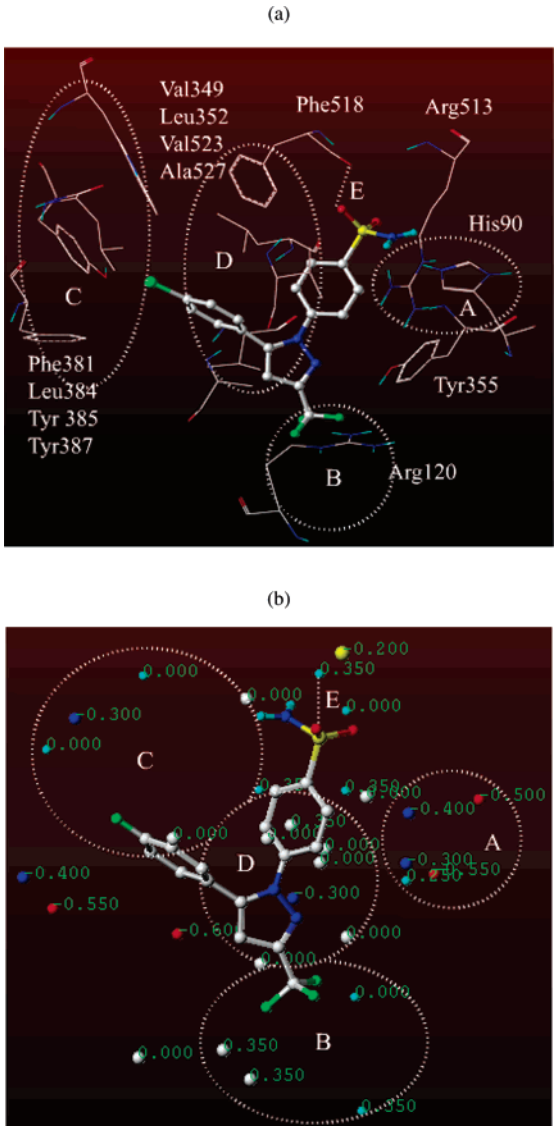

Figure 11. (a) The final binding mode of **5** inside the FLARM 2.0 model. All the receptor atoms are labeled with atomic charges. (b) The binding mode of **SSC-558** inside binding site of COX-2 (PDB code 1CX2). Only the residues that contribute to the binding are displayed for clarity.

(A, B, C, and D) in Figure 11 (parts a and b, respectively), to roughly represent four important regions, and a dashed line E in Figure 11 (parts a and b, respectively) to mark a hydrogen bonding region. It is found the A, B, C, D, and E marked regions of Figure 11a are similar to the regions of Figure 11b marked with the same letter.

A region: There are several hydrogen bond acceptor atoms and donor atoms in the FLARM receptor model, which correspond well with the hydrogen bond acceptor atoms and donor atoms of COX-2's His 90 and Arg 513. In the crystal structure, the NH_2 group of **SSC-558** can form one or two hydrogen bonds with these residues. Unfortunately, in the FLARM models, the NH_2 group of **5** adopts an opposite orientation, forming only a weak hydrogen bond with a sulfur atom of the receptor mode, while strong hydrogen bonds are not formed. As mentioned above, the sulfonamide moieties of all the molecules adopt an orientation that is opposite to that of the crystal structure. FLARM 2.0 failed to rotate them back to the crystal structure orientation to form the hydrogen bonding since local minimization like the Powell algorithm usually cannot rotate a bond nearly 180 degrees. This is a deficiency of FLARM 2.0 that was previously discussed in this paper. However, the A region predicted by FLARM 2.0 is still quite similar to the A region of the crystal structure.

B region: The CF_3 group of **5** forms a strong electrostatic interaction with the charged carbon atoms of the FLARM model, which corresponds well with the crystal structure which indicates that the CF_3 group of **SSC-558** forms a strong electrostatic interaction with the carbamidine group of Arg 120.

C region: The FLARM model has several hydrophobic carbon and hydrogen atoms, which correspond with the hydrophobic residues Phe 381, Leu 384, Tyr 385, and Tyr387 of COX-2 in the same region.

D region: D region is also a hydrophobic interaction region. In this region the FLARM model also has several hydrophobic carbon and hydrogen atoms, which correspond with the hydrophobic residues Val 341, Leu 352, Phe 518, Val 523, and Ala527 of COX-2 in the same region.

E region: An important and strong hydrogen bond (marked as E in Figure 11b) form in the FLARM 2.0 model, which corresponds well with the hydrogen bond in the crystal structure (also marked as E in Figure 11a).

In summary, the FLARM 2.0 pseudoreceptor mimics the binding site of COX2 quite well, especially for the regions in which hydrogen bonding or electrostatic interaction is important. FLARM 2.0 does not explicitly calculate the hydrophobic interaction energy since the hydrophobic interactions are complicated; however, it seems that the mimicking of the hydrophobic regions of COX2 is acceptable, though not so prominent.

Further Discussion on the Method. Generally, the concept of current 4D-QSAR in drug design refers to the extension from 3D to 4D by allowing for a multiconformational representation of the ligand molecules.[30] For example, Hopfinger et al. proposed the 4D-QSAR formalism that incorporates conformational and alignment freedom into the development of 3D-QSAR models as the fourth dimension.[31] Guccione et al. proposed a kind of multiconformer technique: each molecule in the data set was represented by five separate low-energy conformers, and then all of them were used in the generation of HASL 3D-QSAR models.[32] By allowing for a multiconformational representation of the ligand molecules, Vedani and co-workers updated their Quasar model from 3D to 4D[33,34] (and even to 5d by allowing for a multiple representation of induced-fit hypotheses[35,36]). Compared to these methods, FLARM 2.0 cannot be regarded as a full 4D-QSAR method since the ligand is only locally minimized and the conformers produced are not diverse enough. However, FLARM 2.0 has some 4D-QSAR properties by using a flexible-ligand strategy and practically improves the quality of 3D-QSAR. An advantage of the flexible-ligand strategy is that it may be more predictive since by using the multiple-conformer strategy it is hard to select a proper conformer for prediction. The robustness and predictive ability of FLARM 2.0 were proved by the above case studies. FLARM 2.0 is also easy to use. It can easily be used as a 3D-QSAR method while providing users with additional fourth-dimensional information.

The idea of an open receptor model makes FLARM models simple, concise, less noisy, and easy for analysis.

The FLARM receptor models often correspond well with pharmacophore models and/or the binding sites of the real protein receptors. It is also found that the final conformations and alignments of the molecules created by FLARM 2.0 are similar to the receptor-based conformations and alignments. Using the conformations and alignments created by FLARM 2.0, one can usually obtain better 3D-QSAR results than the original results. In our three case studies, all the CoMFA and FLARM 1.0 results improved when FLARM 2.0 conformations and alignments were used (some of these results are not presented in the interest of length). One might argue that by using a field-fit strategy the quality of 3D-QSAR models can also improve. We have tried to apply the field-fit method of SYBYL to the three systems; however, only the steroid system showed improvement for the CoMFA studies. For the GABA receptor inhibitors, two sets of bioactivity data (fly and rat) were available. FLARM 2.0 can produce two respective sets of conformations and alignments for the two data sets, but we do not know how to produce two sets of conformations and alignments that are respectively proper for different data sets by using the field-fit method of SYBYL. It is also worth pointing out that the flexible docking of the ligand inside the receptor model is only a process to optimize the pose of the ligand to achieve minimal docking energy, rather than to adjust the pose of the ligand to get good statistical results. So the FLARM 2.0 produced conformations and alignments are not the results of "high r^2 or q^2 guided fitting".

Though not a severe problem since the computational ability of computers is ever increasing, the computational time of a FLARM run is not short. The other main deficiency of the method is that the docking is not globally minimized, which means that the starting conformations and the alignment of the molecules are still important. Users are encouraged to carefully prepare their molecules as they do in the conventional 3D-QSAR studies. FLARM 2.0 is indeed tolerant of errors or uncertainties of the molecules, but this ability is still limited. A more global and deterministic optimization algorithm will be implemented in the next version of FLARM to make it a real 4D-QSAR method. Furthermore, the flexibility of the receptor upon binding is also a direction for improvement.

CONCLUSION

We have developed the FLARM 2.0 method to relieve the errors and uncertainties caused by the molecular conformation and alignment problems in the 3D-QSAR. In the analysis of the three case studies, FLARM 2.0 shows a number of advantages including conciseness, ease of use, robustness, and highly predictive ability. FLARM 2.0 pseudoreceptor models can correspond well with the pharmacophore models and/or the binding sites of the real protein receptors.

ACKNOWLEDGMENT

This work was supported by the State Key Program of Basic Research of China (2003CB715900), the High-Tech Program of China, and the National Natural Science Foundation of China (20228306, 30490240, 90403001). We thank Julia Liu at Princeton University for her revision of the manuscript.

REFERENCES AND NOTES

(1) Jain, A. N.; Dietterich, T. G.; Lathrop, R. H.; Chapman, D.; Critchlow, R. E.; Bauer, B. E.; Webster, T. A.; Lozano-Perez, T. A shape-based machine learning tool for drug design. *J. Comput.-Aided Mol. Des.* **1994**, *8*, 635−652.

(2) Walters, D. E.; Hinds, R. M. Genetically evolved receptor models: A computational approach to construction of receptor models. *J. Med. Chem.* **1994**, *37*, 2527−2536.

(3) Hahn, M. Receptor surface models. 1. Definition and construction. *J. Med. Chem.* **1995**, *38*, 2080−2090.

(4) Hahn, M. Receptor surface models. 2. Application to quantitative structure−activity relationships studies. *J. Med. Chem.* **1995**, *38*, 2091−2102.

(5) Vedani, A.; Zbinden, P.; Snyder, J. P.; Greenidge, P. A. Pseudoreceptor modeling: The construction of three-dimensional receptor surrogates. *J. Am. Chem. Soc.* **1995**, *117*, 4987−4994.

(6) Vedani, A.; Zbinden, P. Quasi-atomistic receptor modeling. A bridge between 3D-QSAR and receptor fitting. *Pharm. Acta Helv.* **1998**, *73*, 11−18.

(7) Chen, H. M.; Zhou, J. J.; Xie, G. PARM: A genetic evolved algorithm to predict bioactivity. *J. Chem. Inf. Comput. Sci.* **1998**, *38*, 243−250.

(8) Pei, J. F.; Zhou, J. J.; Xie, G. R.; Chen, H. M.; He, X. F. PARM: A practical utility for drug design *J. Mol. Graphics Modell.* **2001**, *19*, 448−554.

(9) Pei, J. F.; Zhou, J. J. Flexible atom receptor model. *Acta Chim. Sin.* **2002**, *60*, 973−979.

(10) Peng, T.; Pei, J. F.; Zhou, J. J. 3D-QSAR and receptor modeling of tyrosine kinase inhibitors with flexible atom receptor model (FLARM). *J. Chem. Inf. Comput. Sci.* **2003**, *43*, 298−303.

(11) Lu, A. J.; Zhou, J. J. Pseudoreceptor models and 3D-QSAR for imidazobenzodiazepines at $GABA_A$/BzR subtypes $\alpha_x\beta_3\gamma_2$ [x=1−3, 5, and 6] via flexible atom receptor model. *J. Chem. Inf. Comput. Sci.* **2004**, *44*, 1130−1136.

(12) Shen, B.; Lu, Z. H.; Chi, X. B.; Lv, H. F.; Ren, T. R. Pseudoreceptor models for inhibitors at GABA receptor via flexible atom receptor model. *Acta Phys.-Chim. Sin.* **2005**, *21*, 800−803.

(13) Wang, R. X.; Lai, L. H.; Wang, S. M. Further development and validation of empirical scoring functions for structure-based binding affinity prediction. *J. Comput.-Aided. Mol. Des.* **2002**, *16*, 11−26.

(14) Brooks, B. R.; Bruccoleri, R. E.; Olafson, B. D.; States, D. J.; Swaminathan, S.; Karplus, M. CHARMM: A Program for Macromolecular Energy, Minimization, and Dynamics Calculations. *J. Comput. Chem.* **1983**, *4*, 187−217.

(15) *SYBYL, version 6.91*; Tripos Associates: St. Louis, MO, 2004.

(16) Wang, R. X.; Fang, X. L.; Lu, Y. P.; Wang, S. M. The PDBbind database: Collection of binding affinities for protein−ligand complexes with known three-dimensional structures. *J. Med. Chem.* **2004**, *47*, 2977−2980.

(17) Cramer, R. D., III; Patterson, D.E; Bunce, J. D. Comparative molecular field analysis (CoMFA). 1. Effect of shape on binding of steroids to carrier proteins. *J. Am. Chem. Soc.* **1988**, *110*, 5959−5967.

(18) Liu, H.; Huang, X. Q.; Shen, J. H.; Luo, X. M.; Li, M. H.; Xiong, B.; Chen, G.; Shen, J. K.; Yang, Y. M.; Jiang, H. L.; Chen, K. X. Inhibitory mode of 1,5-diarylpyrazole derivatives against cyclooxygenase-2 and cyclooxygenase-1: Molecular docking and 3D-QSAR analyses. *J. Med. Chem.* **2002**, *45*, 4816−4827.

(19) Klebe, G.; Abraham, U.; Mietzner, T. Molecular similarity indices in a comparative analysis (CoMSIA) of drug molecules to correlate and predict their biological activity. *J. Med. Chem.* **1994**, *37*, 4130−4146.

(20) Kearsley, S. K.; Smith, G. M. An alternative method for the alignment of molecular structures: maximizing electrostatic and steric overlap. *Tetrahedron Comput. Method.* **1990**, *3*, 615−633.

(21) Ozoe, Y.; Mochida, K.; Nakamura, M.; Akamatsu, M.; Miyake, T.; Matsumura, F. Fipronil-related heterocyclic compounds: structure−activity relationships for interaction with γ-aminobutyric acid and voltage-gated ion channels and insecticidal action. *Pestic. Biochem. Physiol.* **2000**, *66*, 92, 92−104.

(22) Ozoe, Y.; Niina, K.; Matsumoto, K.; Ikeda, I.; Mochida, K.; Ogawa, C.; Matsno, A.; Miki, M.; Yanagi, K. Actions of cyclic esters, S-esters, and amides of phenyl- and phenylthiophosphonic acids on mammalian and insect GABA-gated chloride channels. *Bioorg. Med. Chem.* **1998**, *6*, 73−83.

(23) Hamano, H.; Nagata, K.; Fukada, N.; Shimotahira, H.; Ju, X. L.; Ozoe, Y. 5-[4-(3,3-Dimethylbutoxycarbonyl)phenyl]-4-pentynoic acid and its derivatives inhibit ionotropic gamma-aminobutyric acid receptors by binding to the 4′-ethynyl-4-*n*-propylbicycloorthobenzoate site. *Bioorg. Med. Chem.* **2000**, *8*, 665−674.

(24) Ren, T. R.; Shen, B.; Pei, J. F.; Wang, Y. S.; Xiang, W. S. Pharmacophore models and 3D-QSAR studies of rat and fly's GABA receptor inhibitors. *Chem. J. Chin. Univ.* **2005**, *26*, 546−549.

(25) Morris, G. M.; Goodsell, D. S.; Halliday, R. S.; Huey, R.; Hart, W. E.; Belew, R. K.; Olson, A. J. Automated docking using Lamarckian

genetic algorithm and empirical binding free energy function. *J. Comput. Chem.* **1998**, *19*, 1639−1662.
(26) Datar, P. A.; Coutinho, E. C. A CoMFA study of COX-2 inhibitors with receptor based alignment. *J. Mol. Graphics Modell.* **2004**, 23, 239−251.
(27) Wang, R. X.; Liu, L.; Lai, L. H.; Tang, Y. Q. SCORE: A new empirical method for estimating the binding affinity of a protein−ligand complex. *J. Mol. Mod.* **1998**, *4*, 379−394.
(28) Pei, J. F.; Wang, Q.; Zhou, J. J.; Lai, L. H. Estimating protein−ligand binding Free energy: Atomic solvation parameters for partition coefficient and solvation free energy calculation. *Proteins* **2004**, *57*, 651−664.
(29) Pei, J. F.; Wang, Q.; Liu, Z. M.; Li, Q. L.; Yang, K.; Lai, L. H. PSI-DOCK: towards highly efficient and accurate flexible ligand docking. *Proteins* **2005**, in press.
(30) Müller, G.; nD QSAR: A medicinal chemist's point of view. *Quant. Struct.-Act. Relat.* **2002**, *21*, 391−396.
(31) Hopfinger, A. J.; Wang, S.; Tokarski, J. S.; Jin, B. Q.; Albuquerque, M.; Madhav, P. J.; Duraiswami, C. Construction of 3D-QSAR models using 4D-QSAR analysis formalism. *J. Am. Chem. Soc.* **1997**, *119*, 10509−10524.
(32) Guccione, S.; Doweyko, A. M.; Chen, H.; Barretta, G. U.; Balzano, F. 3D-QSAR using 'Multiconformer' alignment: The use of HASL in the analysis of 5-HT1A thienopyrimidinone ligands. *J. Comput.-Aided Mol. Des.* **2000**, *14*, 647−657.
(33) Vedani, A.; Briem, H.; Dobler, M.; Dollinger, K.; McMasters, D. R. Multiple conformation and protonationstate representation in 4D-QSAR: The neurokinin-1 receptor system. *J. Med. Chem.* **2000**, *43*, 4416−4427.
(34) Vedani, A.; McMasters, D. R.; Dobler, M. Multiconformational ligand representation in 4D-QSAR: Reducing the bias associated with ligand alignment. *Quant. Struct.-Act. Relat.* **2000**, *19*, 149−161.
(35) Vedani, A.; Dobler, M. 5D-QSAR: The key for simulating induced fit? *J. Med. Chem.* **2002**, *45*, 2139−2149.
(36) Vedani, A.; Dobler, M. Multidimensional QSAR: Moving from three- to five-dimensional concepts. *Quant. Struct.-Act. Relat.* **2002**, *21*, 382−390.

CI050203C